Available online at www.sciencedirect.com
ScienceDirect
Nuclear Physics B Proceedings Supplement 00 (2014) 1–6
Nuclear Physics B Proceedings Supplement

Measurements of Higgs boson production and properties in the WW decay channel with both W's decaying into electrons or muons plus neutrino using the CMS detector

Pietro Govoni for the CMS Collaboration[a]

[a]*INFN and University of Milano-Bicocca*

Abstract

In the data collected so far at the LHC collider, the CMS experiment measured a strong evidence for a new resonance at an invariant mass of about 125 GeV. The analysis is outlined in its most important aspects, as well as the main results obtained. In fact, this final state allows for a very precise determination of the signal cross-section, and for the investigation of the tensor structure of the resonance decay. Results show that the behaviour of the new particle is compatible with the expectations for a Standard Model Higgs boson.

Keywords:

Introduction

The LHC collider produced proton-proton collisions operating at the centre-of-mass energies of 7 TeV and 8 TeV, when both the CMS and ATLAS detector collected about 5 fb^{-1} of data at the former luminosity and 20 fb^{-1} at the latter. The analysis of these events brought to the discovery, at the two experiments, of a new resonance with mass of about 125 GeV, with properties so far compatible with the Standard Model Higgs boson behaviour.

The CMS community focussed since the very beginning on searches for Higgs boson candidates decaying to vector bosons [1]. In fact, the non-vanishing coupling to vector boson is one of the consequences of the electro-weak symmetry breaking, and the angular distributions of the decay products allowed allowed to test the CP propetries of the decaying resonance. The final state with two W bosons decaying leptonically into electrons or muons features a large expected cross-section and a clear signature, which in the CMS detector [2] is searched for selecting two isolated leptons with opposite charge and transverse momentum of 20 and 10 GeV respectively. The presence of neutrinos in the final state is accounted for by requiring at least 20 GeV of transverse missing energy. The signal can be produced

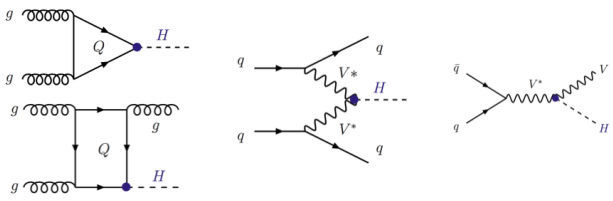

Figure 1: The three main Higgs boson production diagrams at tree level. From left to right: gluon fusion, vector boson fusion and Higgs–strahlung.

mainly through three mechanisms. The most likely is initiated by a pair of gluons, that via a top loop generate the Higgs boson (gluon fusion). The second one is about one order of magnitude less important, and produces the Higgs boson through the fusion of massive vector bosons irradiated by the incoming partons of the collision. In this topology, called vector boson fusion, the two incoming partons most likely deviate from the beam direction and enter the active volume

of the detector, generating two jets that with their presence and kinematic behaviour strongly characterise the event. The third production mechanism happens when a single massive vector boson is produced, and in turn radiates a Higgs boson (Higgs-strahlung). The radiating vector boson is detected as well and helps in isolating the signal. Figure 1 shows the Feynman diagrams for these three processes. To profit from the additional handles present in the vector boson fusion and Higgs-strahlung channels, additional leptons may be allowed by the analysis, as well as additional jets, which are considered only when having transverse momentum larger than 30 GeV. In the harsh environment of a hadron collider the backgrounds to this analysis are due to non-resonant WW production, $t\bar{t}$ and single top production, non-resonant di-boson production where some of the decay products are lost in the reconstruction. In the case of the Ws decay into same flavour leptons, the drell-yan production is an important background as well. Furthermore, the small probability for a hadron-jet to be reconstructed as an isolated lepton, combined with the large production cross-section of single W boson plus jets, lets this channel to pollute the signal region as well.

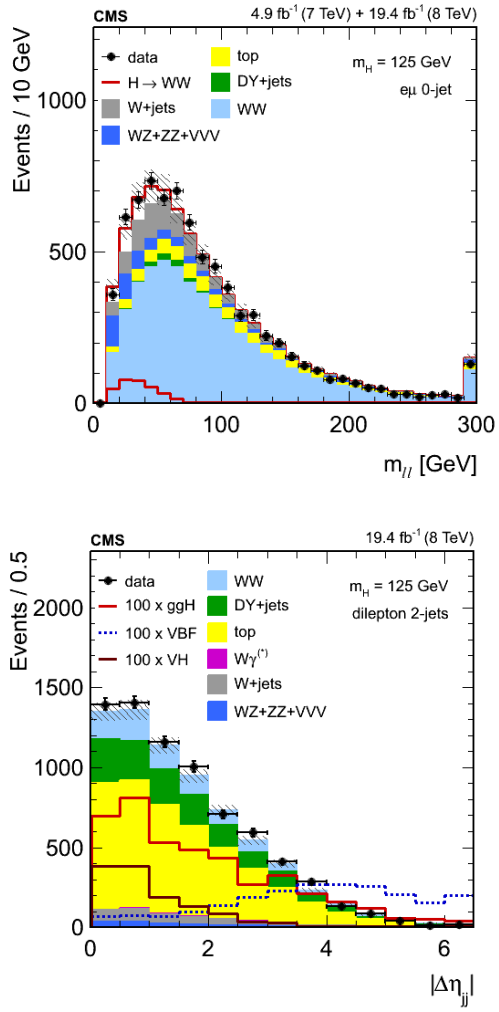

Figure 2: The $m_{\ell\ell}$ distribution for the zero-jet, different-flavour category (top), and the $|\Delta\eta_{jj}|$ one for the vector boson fusion (bottom), after selecting the final state topology of the analysis.

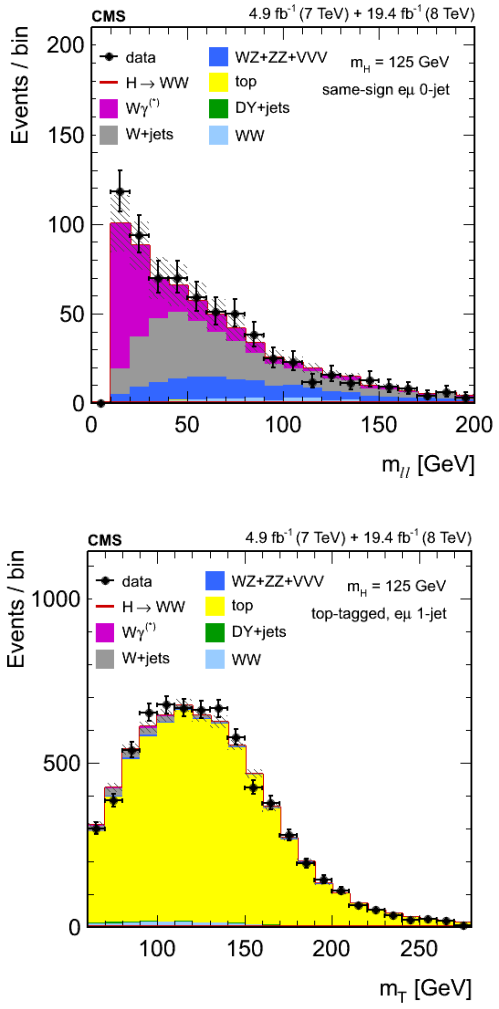

Figure 3: Background-enriched phase spaces: W$\gamma(*)$ sample in the 0-jet bin (top) and top-enriched region in the 1-jet bin (bottom).

1. The events reconstruction

A particle-flow algorithm [3] is used to reconstruct the particles in the event. For each event, clusters of

energy depositions measured by the calorimeters and charged-particle tracks identified in the central tracking system and the muon detectors are combined to reconstruct individual particles and to set quality criteria to select and define final-state observables. When possible, particles are required to originate from a single primary vertex, identified as the one producing the largest p_T^2 flux in the detector. Electron candidates are defined by a reconstructed charged-particle track pointing to a cluster of energy deposition in the electro-magnetic calorimeter. Their energy is determined combining the calorimetric and tracking information, as generally the tracking resolution is worse than the calorimetric one, conversely to what happens at low energies, where the combination of the two measurements improves the overall precision. Muon candidates are identified by charged-particle tracks in the muon system compatible with a track reconstructed in the central tracking detector. Uncertainties in the lepton momentum scale and resolution are 0.54% per lepton, and the effect on the yields at the analysis selection level is approximately 2% for electrons and 1.5% for muons. Electrons and muons are required to be isolated to reject leptons from QCD production or misidentification, usually situated inside or near jets of hadrons. A correction is applied to the neutral component in the isolation cone based on the average energy density deposited by the neutral particles from additional interactions [4], while the vertex requirement suppresses the charged component of the pile-up contamination. Jets are reconstructed using the anti-kT clustering algorithm [5] with a distance parameter of 0.5, as implemented in the fastjet package [6, 7]. The pile-up subtraction is applied in a similar way to the lepton isolation case, and a dedicated selection variable has been implemented to discard jets generated by the clustering of pile-up deposits only. Bottom quarks are tagged by the presence of a soft-muon in the event and by identification criteria based on the impact parameter of the constituent tracks [8]. The missing transverse energy (MET) vector is defined as the negative vector sum of the reconstructed particles transverse momenta in the event. The projection of this vector onto the nearest lepton (if the lepton is closer than $\pi/2$ in the transverse plane to the MET) is used to reject the $Z \to \tau\tau$ background. Finally, to minimise the impact of pile-up, the missing transverse energy is reconstructed also by using charged particles only, and the minimum between the two possible MET values is used in the analysis: in the following, the missing transverse energy will identify this last variable.

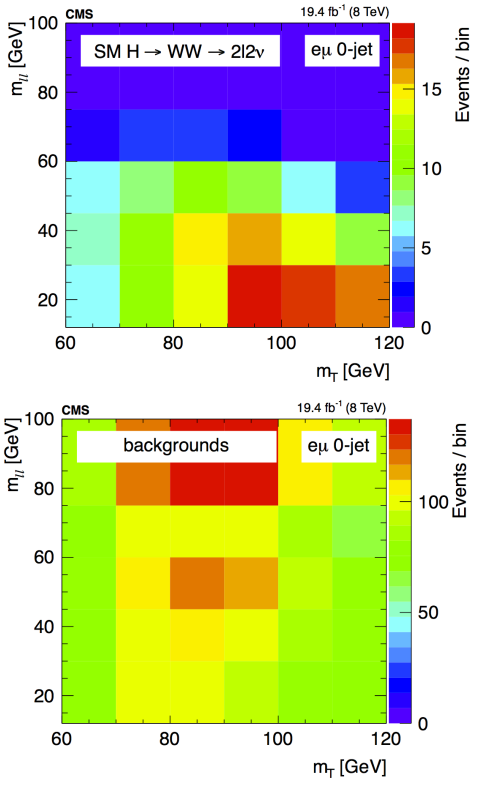

Figure 4: The (m_T, $m_{\ell\ell}$) plane for signal and background models, in the 0-jet different flavour bin.

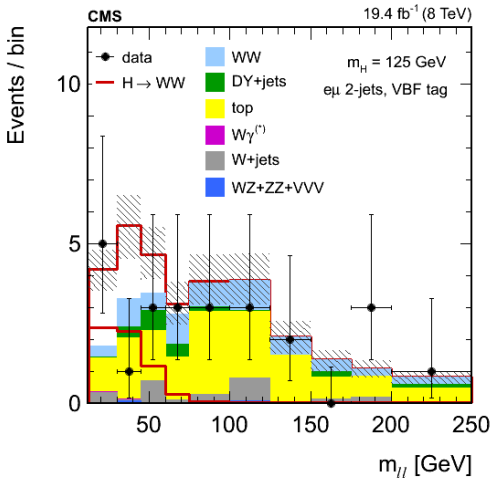

Figure 5: The $m_{\ell\ell}$ distribution in the vector boson fusion case, before the final fit.

2. The data analysis selection

Events are categorised into sub-sets with different signal purity. Events with two same-flavour and

different-flavour leptons are treated separately, and each of the two sets is further divided according to the number of jets. The sets with 0 and 1 additional jets contain mostly events produced through gluon fusion, while the one with two additional jets contains mostly signal events produced through vector boson fusion or bremsstrahlung. The latter is also searched for with events featuring three charged leptons in the final state. In each category, additional selections are applied to optimise the analysis potential. In the case of exactly

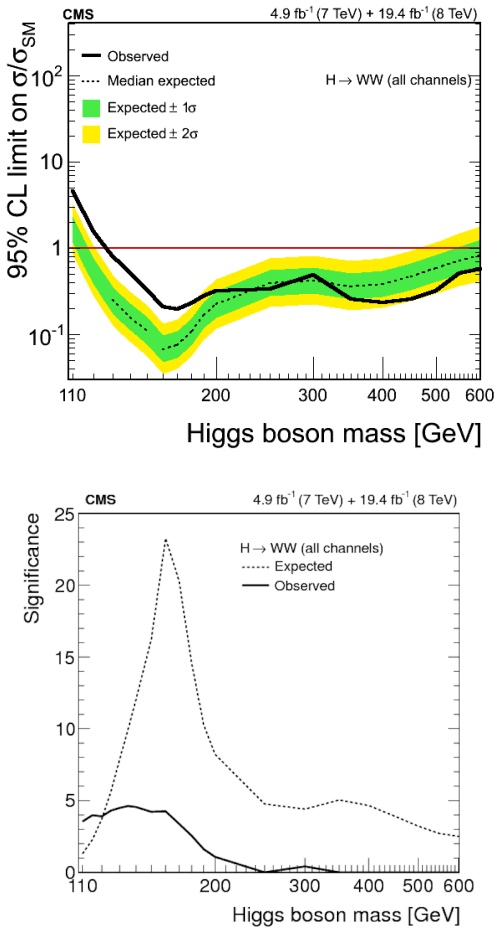

Figure 6: The Standard Model Higgs boson exclusion limit (left) and discovery significance (right) for the combination of all the analysed channels.

two oppositely charged leptons events contain a missing transverse energy of at least 20 GeV, and satisfy $m_{\ell\ell} > 12$ GeV, $p_T^{\ell\ell} > 30$ GeV and $m_T > 30$ GeV, where the transverse mass is defined as $m_T^2 = 2p_T^{\ell\ell}E_T^{miss}(1 - \cos\Delta\phi(\ell\ell, \vec{E}_T^{miss}))$. Top-tagged events are vetoed, to suppress the $t\bar{t}$ and single top production. In the case of same flavour leptons, additional selections suppress the Drell-Yan background: $m_{\ell\ell}$ is more than 15 GeV away from the Z boson mass, together with a combination of selections based on missing transverse energy, and kinematical and topological requirements on the final state objects. The two-jet category addresses the vector boson fusion production, where the two additional jets are expected to have a large separation in η and a large invariant mass. Therefore, the two highest p_T jets satisfy the following selections: $m_{jj} > 500$ GeV and $|\Delta\eta_{jj}| > 3.5$. Finally, events with an additional jet situated in the pseudorapidity range between the two leading jets are rejected, and both leptons are required to be within the pseudorapidity region defined by those jets. While for the zero-jet category the most important background is due to the non-resonant WW production, in the two-jets case it is due by processes with top quarks, and the one-jet category shares the two. If the two additional jets have an invariant mass in the range (65 GeV, 105 GeV), the event is categorised separately and further selections are put in place to isolate the bremsstrahlung topology. Also in this case, the top sample is the dominating background source. The three-lepton category also addresses the same production channel, which is studied separately as WH$\rightarrow 3\ell 3\nu$ and ZH$\rightarrow 3\ell\nu + 2$ jets. The on-resonant WZ production and the tri-boson one are the principal sources of background in this cases.

Figure 2 shows as an example the $m_{\ell\ell}$ distribution for the zero-jet, different-flavour category at the top, and the $|\Delta\eta_{jj}|$ one for the vector boson fusion at the bottom. Already at this level of selections, the Higgs signal is clearly visible on top of the backgrounds, as well as the different shapes of the two. The amount of basically all the backgrounds still contaminating the signal region is measured in enriched regions, so to guarantee a fully data-driven approach to the analysis. Figure 3 shows as an example two background-enriched phase spaces. On the left, the same charge leptons pair sample used in the zero-jet, different-flavour category to determine the W$\gamma(*)$ contribution is reported, while on the right the top-enriched region in the one-jet different flavour category is shown. As an example, in the two-leptons, zero- and one-jet cases the WW background is normalised on data in signal-free regions, and the $t\bar{t}$ is determined by rescaling a top-enriched region with the top-tagging efficiency, measured on data as well. The instrumental W+jets background, where a jet is mis-identified as a lepton, is determined by measuring the probability of a jet to be mis-identified, ad extrapolating from a region with a loosely identified lepton.

The backgrounds distributions and the expected sig-

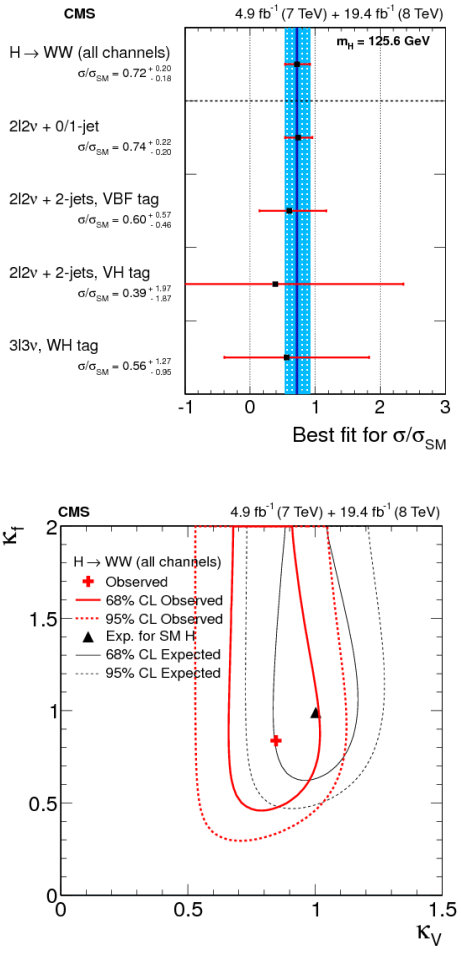

Figure 7: Discovery significances for the analysis sub-channels at m_H = 125.6 GeV (left), and two-dimensional likelihood profiles of a fit in the (κ_V, κ_f) plane.

nal ones are then compared to data in the various categories, to search for a signal candidate in the Higgs boson mass range from 110 GeV to 600 GeV. Depending on the category, either a two-dimensional fit, a one-dimensional fit or a cut-and-count approach is followed, to distinguish the signal-and-background hypothesis from the background-only one. For example, the two-leptons, different-flavour zero- and one-jet categories feature a 2D fit based on the m_T and $m_{\ell\ell}$ variables, while the vector boson fusion events are fit along $m_{\ell\ell}$ only. Figure 4 shows the (m_T, $m_{\ell\ell}$) plane for the signal and for the sum of all the backgrounds, where it is apparent that the signal is peaking at large m_T and low $m_{\ell\ell}$. Here, the uncertainty on the signal efficiency is about 20%, due to theoretical uncertainties, while the one on the background is mostly due to the statistical fluctuations in the control regions, and theoretical uncertainties on the non-resonant WW background. The

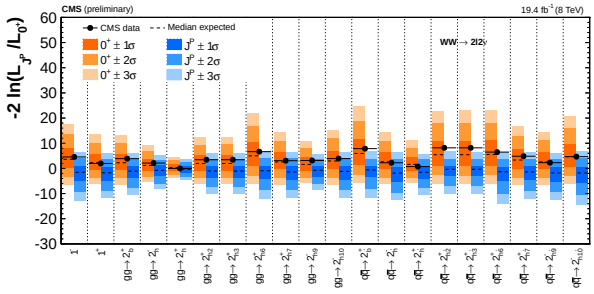

Figure 8: Likelihood ratio distribution for Standard Model case (orange) and for alternative spin hypotheses (blue) for the new resonance spin characterisation.

presence of two neutrinos in the final state does not allow to measure the mass precisely, while the large branching ratio of the 125.6 GeV Higgs boson into WW renders this channel very accurate in the cross-section measurement, which is determined to be, in this category, 0.76 ± 0.21 times the expected Standard Model value. Figure 5 shows as an example the $m_{\ell\ell}$ distribution in the vector boson fusion case. The expected contribution for a Higgs boson signal with m_H = 125 GeV (red line) is also shown, both separately and stacked with the background histograms.

3. The results of the data analysis

The combined 95% confidence level upper limits on the production cross section of the Higgs boson are shown in Figure 6, on the left-hand side. The excess of events observed for a low mass hypothesis makes the observed limit weaker than the expected one, and the Standard Model Higgs boson results excluded at the 95% confidence level in the mass range 127-600 GeV only. The expected and observed significances for the Standard Model Higgs boson as a function of the mass hypothesis for each category and for the combination are shown on the right-hand side of the Figure. With an expectation of 5.8 standard deviations at the Higgs boson mass of 125.6 GeV, the observed one is 4.3. This corresponds to a signal strength, $\sigma/\sigma_{\rm SM}$, of $0.72\,^{+0.20}_{-0.18} = 0.72\,^{+0.12}_{-0.12}(\text{stat.})\,^{+0.12}_{-0.10}(\text{th. syst})^{+0.10}_{-0.10}(\text{exp. syst})$. Figure 7 shows, on the left-hand side, the signal strength separately for the various analysis categories, where the various results are clearly compatible among

themselves. The categorisation of the events into final states sensitive to different production mechanisms, allows to perform a fit, keeping the Higgs couplings to fermions and vector bosons independent with respect to one another. Figure 7 shows, on the right-hand side, the two-dimensional likelihood profiles of a fit, where the coupling of the Higgs boson to vector bosons is rescaled by a factor κ_V, and the one to fermions by a factor κ_f. The observed minimum is compatible with the Standard Model expectations within the one standard deviation contour.

The observables used in the analysis, such as the opening angle between the two reconstructed leptons in the transverse plane, the dilepton invariant mass, and the transverse mass, are sensitive to the tensor structure of a Higgs boson decaying to two gauge bosons. By means of binned maximum likelihood fits to the selected events, anomalous couplings in the spin-zero configuration have been measured, and proven to be in agreement with the Standard Model expectations. Furthermore, hypotheses with a spin-1 and spin-2 Higgs boson have been tested as well: in all cases the data favours the Standard Model hypothesis with respect to the alternative one, as shown in Figure 8 Here, for each model the coloured bands represent the 1, 2 and 3 standard deviation bands around the value of the likelihood ratio, for the Standard Model case in orange and for the alternative hypothesis in blue. Black points represent the observed value.

Conclusions

In conclusion, in the LHC data collected so far the CMS experiment measured a strong evidence for a new resonance at an invariant mass of about 125 GeV, in the fully-leptonic WW decay channel. Despite the low resolution in the invariant mass, the large signal yield renders this channel very precise in the cross-section measurement. Its properties have been thoroughly investigated and, within the uncertainties attained by the analysis, the behaviour of the new particle is compatible with the expectations for a Standard Model Higgs boson.

References

[1] S. Chatrchyan *et al.* [CMS Collaboration], JHEP **1401** (2014) 096 [arXiv:1312.1129 [hep-ex]].
[2] S. Chatrchyan *et al.* [CMS Collaboration], JINST **3** (2008) S08004.
[3] S. Chatrchyan *et al.* [CMS Collaboration], CMS-PAS-PFT-09-001 (2009).
[4] M. Cacciari and G. P. Salam, Phys. Lett. B **659** (2008) 119 [arXiv:0707.1378 [hep-ph]].
[5] M. Cacciari, G. P. Salam and G. Soyez, JHEP **0804** (2008) 063 [arXiv:0802.1189 [hep-ph]].
[6] M. Cacciari, G. P. Salam and G. Soyez, Eur. Phys. J. C **72** (2012) 1896 [arXiv:1111.6097 [hep-ph]].
[7] M. Cacciari and G. P. Salam, Phys. Lett. B **641** (2006) 57 [hep-ph/0512210].
[8] S. Chatrchyan *et al.* [CMS Collaboration], JINST **8** (2013) P04013 [arXiv:1211.4462 [hep-ex]].